

# **Anomalous Small angle x-ray scattering of iron-carbides**

**Leonard Zippelius**

University of Edinburgh

**Supervisor: Dr. Ulla Vainio**

DESY Hamburg, Hasylab

# **Table of contents**

1 Abstract

2 Experimental set up

3 Measurements and analysis

3.1 samples

3.2 power law fit

3.3 Algorithm for finding the q range

4 Results

4.1 single energy

4.2 difference of energy curves

5 Conclusion

6 References

## **1) Abstract**

In the project iron-carbides were investigated by the means of anomalous small-angle X-ray scattering (ASAXS). The intensity was measured as a function of the scattering vector for two different energies 6856 eV and 7105 eV, which are close to the absorption edge of iron. Then a power law was fitted to the intensity curves measured at both energies as well as the difference of the intensities measured at the two energies. It was found that the intensity follows a power law with an exponent of -2.428(4).

## **2) Experimental set up**

The investigation of the iron-carbides was done at the research facility DESY in Hamburg at beamline B1. This beamline has been a dedicated ASAXS beamline in operation since 1987 and has therefore the standard SAXS setup which is quickly described in the following paragraph.

At beamline B1 the radiation from DORIS III, a synchrotron storage ring operated with positrons is used as an x-ray source. The white beam is cut to  $3 \text{ mm} \times 1.8 \text{ mm}$  size using horizontal and vertical slits. The beam then goes through a double crystal monochromator (Si(311)) before it encounters an aperture slit to cut the beam further to the desired size  $0.8 \text{ mm} \times 0.5 \text{ mm}$  and further down the beamline a third set of slits, the guard slits, take out the scattering from earlier slits. Shortly behind the last slit the beam is then scattered by the sample. The scattered photons are measured by a Pilatus 1M or Pilatus 300k single photon counting pixel detector. The distance between the detector and the sample is variable from 885 mm to 3585 mm. Most of the path of the x-ray is in vacuum to avoid scattering or absorption by air. Since in the small-angle regime nearly all materials scatter at least slightly it is very important to make sure to avoid the beam getting into contact with too many materials and to choose these materials according to how much they scatter. Since B1 is a dedicated SAXS beamline it is optimized in this respect.

## **3) Measurements and Analysis**

Small angle x-ray scattering is usually used to determine structures in the nanometer scale. It gives results from a few nanometers up to a maximum of a few hundred nanometers. The

iron-carbides used in the experiment are mainly iron with two different kinds of nanoparticles in them. A power law was fitted to the intensity as a function of  $q=4\pi\sin(\theta)/\lambda$  for x-ray energies of 6856eV and 7105eV and through the difference of the intensity curves measured at the two energies. The bigger nanoparticles are expected to give rise to a power-law background while the smaller carbides are expected to have thin ellipsoidal structure which would give rise to two humps in the measured region. We don't expect to see any other humps or diffraction peaks of the bigger nanoparticles, since they are too big and therefore not in the measured  $q$ -range. Subtracting the two intensity curves could make one of the two nanoparticles more dominant, since the scattering contrast of the nanoparticles can change rapidly at the absorption edge.

### 3.1) Samples:

There were five different states of iron-carbides investigated. They were named Z1, Z2, Z3, Z4 and Z5, where the Z stands for the german word Zustand, which means state. The different states were created under different conditions and/or methods. The samples were about 30 to 40  $\mu\text{m}$  thick. At this thickness the samples don't absorb too much of the beam and multiple scattering is negligible.

### 3.2) Power law fit:

A Python script was written to analyze the data. For a region of roughly 0.05 to 0.4 the data was found to have a  $q$  dependence of the form:

$$I = f + cq^{-\alpha}$$

The data were read in and an estimated value was subtracted from the intensity to take into account the fluorescence which should be roughly constant with respect to the  $q$  vector. The logarithm was taken of both the  $q$  values and the intensity. Afterwards a straight line was fitted through the data to obtain the exponent of the power law. The  $q$  range for the straight line fit and the constant for the fluorescence were chosen manually, since finding an algorithm to choose these parameters was not successful for reasons described in the next subsection.

### 3.3) Algorithm for choosing the $q$ -range:

The main problem with choosing the  $q$ -range automatically was to find a parameter judging how good the range was chosen. In general the idea used was to fit straight lines for all possible  $q$ -ranges with at least 100 data points in it and assign a certain value to the quality of the fit. The natural value to use for this is normalized chi-squared ( $\chi^2/N$ ). However the chi-squared is evaluated by dividing by the error squared.

$$\chi^2 = \sum \frac{(I_i - mq_i - c)^2}{\Delta I_i^2}$$

Since the error was much higher for higher  $q$  values the highest  $q$ -range possible was always chosen. For this the straight-line fit is especially good. However, it is clear that this region is not optimal to determine  $\alpha$  of the power law, since the data itself is of lower quality and less precise.

Alternatively it was possible to use a value similar to chi-squared but not dividing by the error squared. This had as an effect that a very low  $q$ -range was chosen. Again this is not optimal since according to theory the power law of interest is not expected in this region. However the small error obviously had the effect that the data points didn't fluctuate as much as in the higher  $q$ -regime. Thus there seemed to be a reason to take the range at high  $q$ -values namely the quality of the fit and a reason to take the range at low  $q$ -values which improved the quality of the data.

Finally it is possible to use a value like chi-square, but instead of dividing by the error squared dividing by the error to a power between 0 and 2. This was done by choosing the power for one dataset such that a  $q$ -range was chosen which was optimal according to human judgment for this dataset and then this value was fixed. However it turned out that although this worked out better than the other two approaches, for most of the data sets it was still far of the optimum range. The optimal parameter needed for this method changes according to the sample. It was then decided to choose the  $q$  range manually instead.

A second problem with automatizing the process of choosing a range for the fit was the increase of time to run the program. Given parameters for the range the program needed about two seconds to give a result. Letting the program choose the range took up to ten minutes. Although this is not a big problem, it is important to take care that this effect doesn't increase when considering possible other methods to automatize the process of choosing a range.

## 4) Results

### 4.1) Single energy:

Not all the fitted curves can be included in the following discussion of the results. Instead a few graphs will be shown as examples and the complete data will be presented in a table as well as a single graph.

The following graph (figure 1) shows the power law fit for the sample Z2B at energy 6856 eV. It is easily seen that although not perfect the trend seems to agree with the data rather well. The exponent in this particular case is  $-2.37(3)$ . The error of 0.03 has to be considered with care. This is the error coming from the fit of a straight line combined with the error of the data points. It does not take into account any systematic error there might be from the data simply not following a straight line. This systematic error is likely to be higher, especially if not enough care is taken in choosing the fitting region. A rough estimate of the systematic error coming from fitting the wrong function to the data was estimated by changing the  $q$  ranges. It was around  $0.1 \text{ 1/\AA}$  and varied slightly for the different samples.

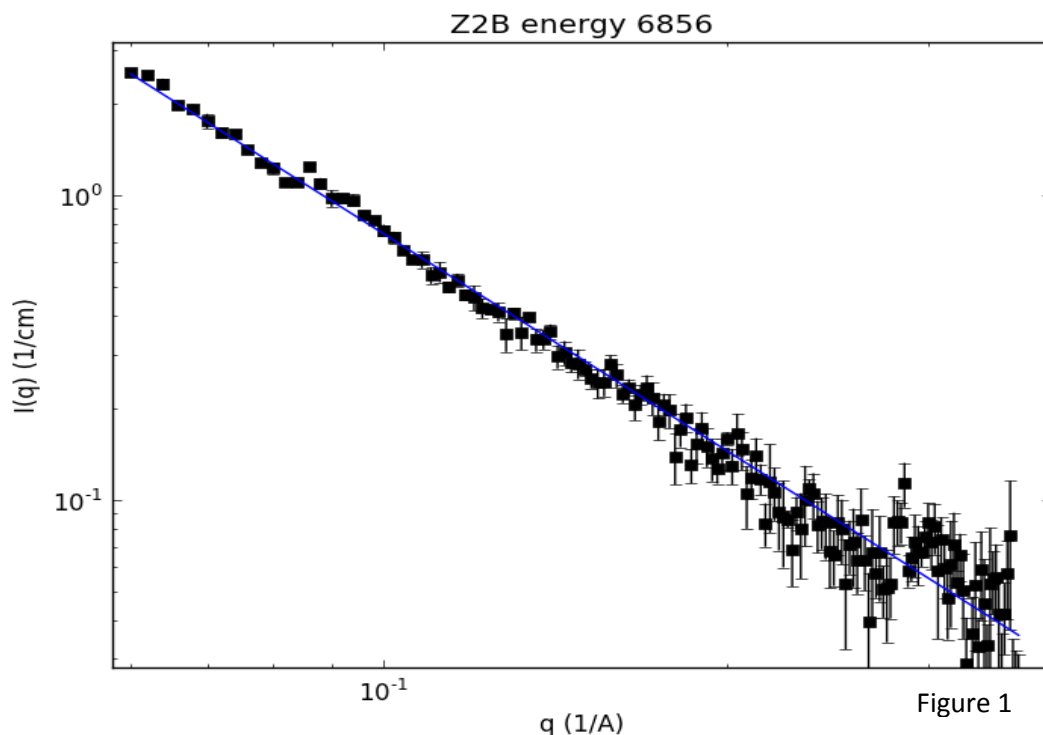


Figure 2 shows the residual plot for Z2B at 6856eV. It is easy to see that although the data might not follow a power law exactly the approximation seems to be rather good. At first glance the residuals seem to be randomly distributed which would be further evidence for the quality of the power law approximation. At a closer look we can see oscillations around the fitted curve. For the lower energy this effect is rather small but for the higher energy the effect in general becomes stronger.

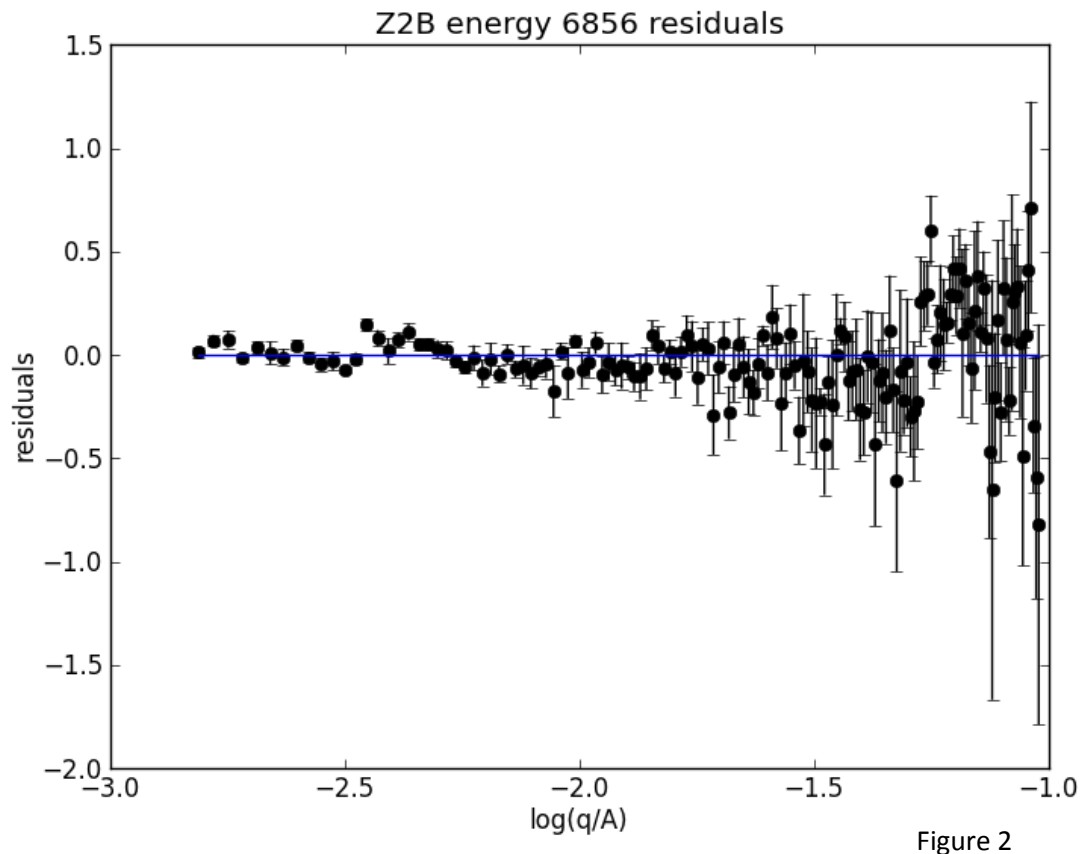
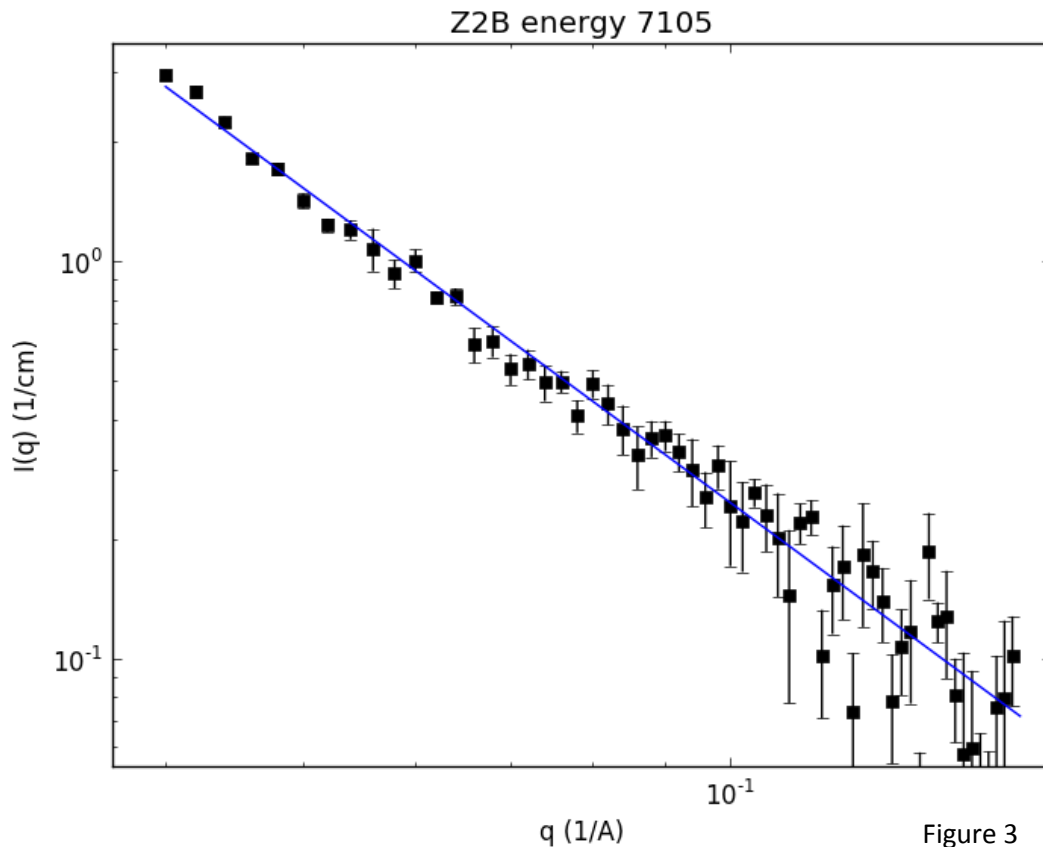


Figure 2

In the following graph we see the same sample for the highest energy at which measurements were done (7105eV). The  $q$  range shown is now much smaller. This is due to the fact that the data simply don't fit the power law as well. Again the data points seem to oscillate around the power law. The effect is the strongest for high  $q$  values. This effect was found for most of the samples at 7105eV. The range therefore needed to be shortened, in order to fit a reasonable power law through the data. These oscillations are possibly just noise. Through the shortening of the range we in general also obtained slightly higher  $\alpha$  then we got when fitting the power law to the data taken at the lower energy.



The following table shows the measurements of the samples at the two energies. The range for which the power law holds is given together with the exponent of the power law.

Sample	Energy	q-range(1/Å)	Range(Å)	$\alpha$	$\Delta \alpha$	$\chi^2/N$
Z1AA	6856	0.01-0.42	2.38-314	2.55	0.02	3.942
	7105	0.1-0.26	3.85-31.4	2.75	0.10	1.049
Z1AB	6856	0.1-0.42	4.17-31.4	2.81	0.03	1.048
	7105	0.04-0.23	4.35-78.5	2.54	0.03	1.906
Z1A	6856	0.0135-0.34	2.94-232.6	2.441	0.05	2.539
	7105	0.0135-0.26	3.84-232.6	2.629	0.04	26.997
Z2B	6856	0.06-0.36	2.78-52.3	2.37	0.03	1.890
	7105	0.04-0.16	6.25-78.5	2.63	0.09	1.876
Z3A	6856	0.06-0.42	2.38-52.3	2.551	0.017	2.576
	7105	0.06-0.26	3.84-52.3	2.48	0.06	1.349
Z3B	6856	0.04-0.4	2.5-78.5	2.383	0.03	1.854
	7105	0.04-0.2	5-78.5	2.009	0.019	41.09
Z4A	6856	0.06-0.42	2.38-52.3	2.616	0.018	3.010
	7105	0.04-0.21	4.76-78.5	2.47	0.04	1.344
Z4B	6856	0.06-0.34	2.94-52.3	2.632	0.014	3.876
	7105	0.04-0.3	3.33-78.5	2.36	0.02	5.266

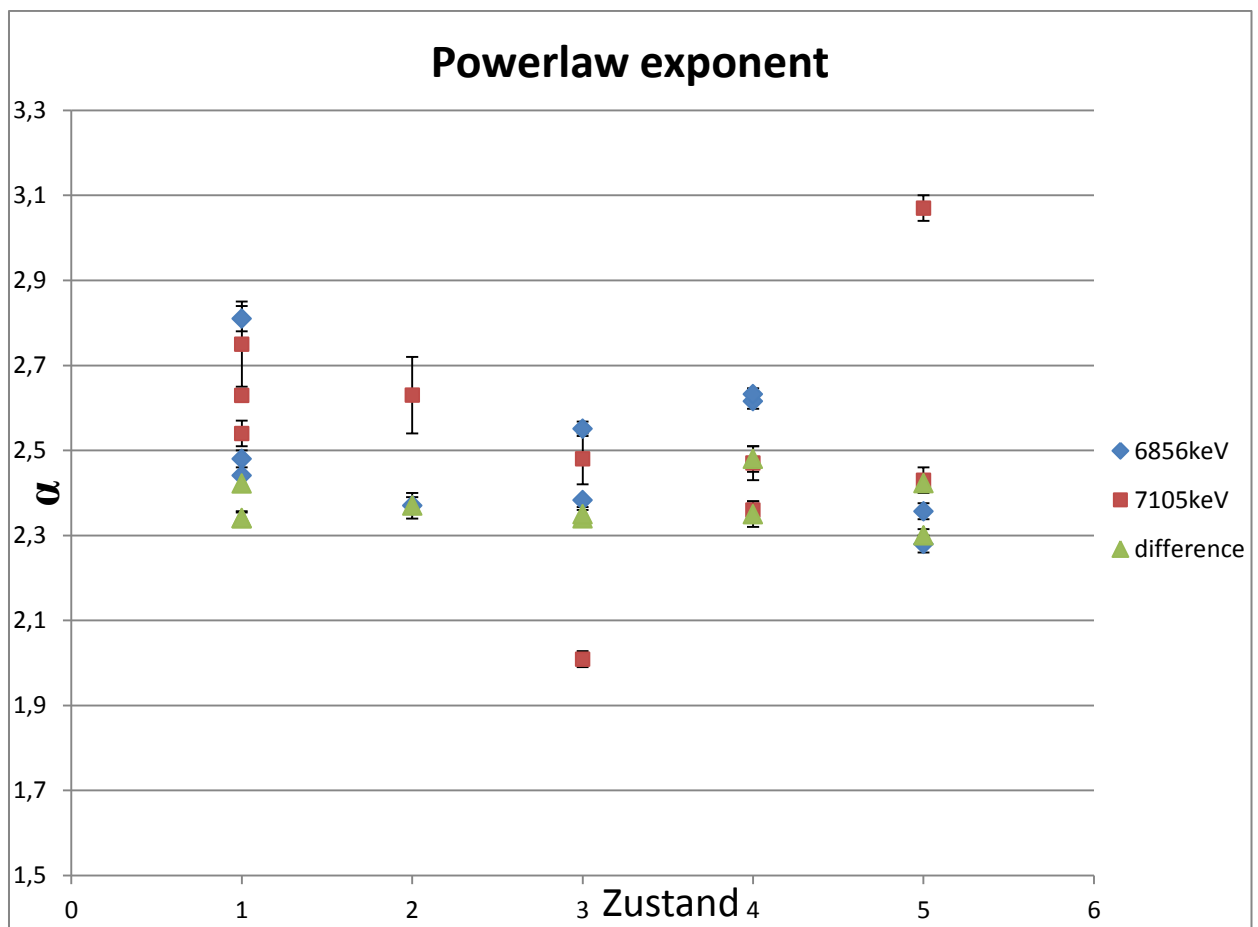
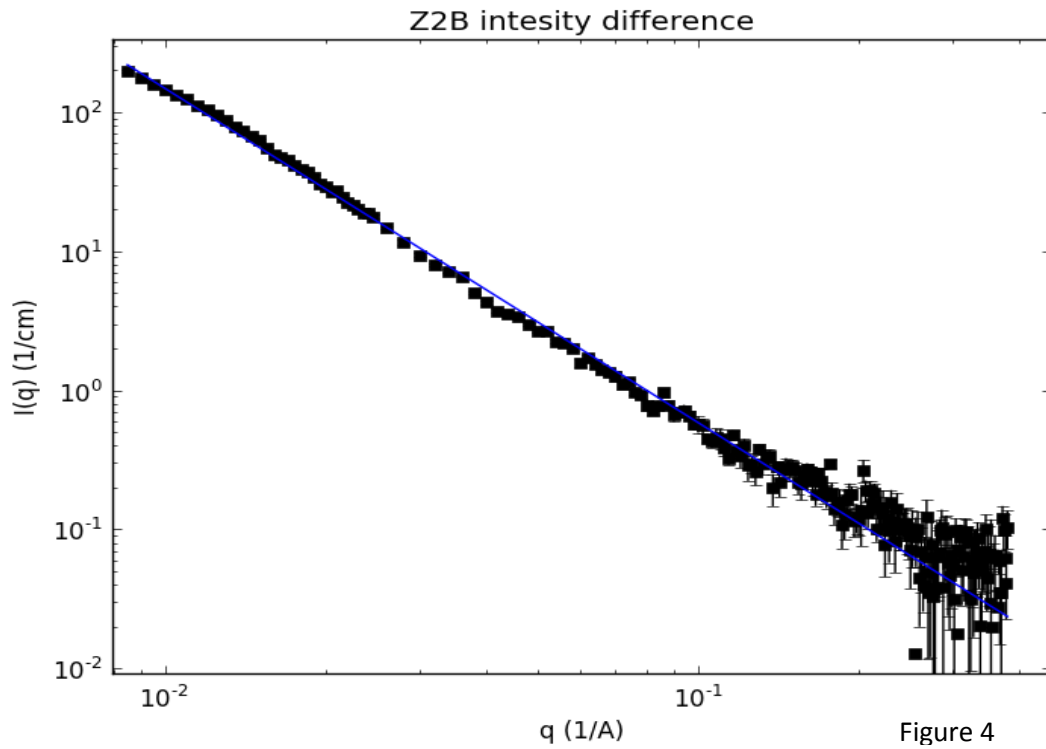


Sample	Energy	q-range (1/Å)	Range(Å)	$\alpha$	$\Delta \alpha$	$\chi^2/N$
Z5A	6856	0.04-0.36	2.78-78.5	2.357	0.019	6.908
	7105	0.0235-0.19	5.26-133.6	3.07	0.03	17.035
Z5B	6856	0.06-0.44	2.27-52.3	2.28	0.02	3.142
	7105	0.04-0.24	4.17-78.5	2.43	0.03	3.929

## 4.2) Difference of energy curves:

Figure 4 shows the difference of the intensity curves at the two energies. It looks like the fit agrees with the data rather well, except for the hump at 0.01-0.02 1/Å. For the difference of the energy curves this was in general the case. The slightly higher chisquared values are understandable. These come from the wide q-range chosen. Since the data seemed to follow a straight line so well it wasn't necessary to exclude the ends. It can be seen that at the ends the straight line fit is not as accurate anymore, but taking these regions barely changed the slope of the line. It did however decrease chi-squared. The hump at roughly  $q=0.01-0.02$  1/Å could be corresponding to the smaller carbides in the sample. However we expected two of these humps, while only one is observed. This hump is cut out of the range for the two single energies, but it was also visible in those datasets. It is slightly enhanced by subtracting the two intensity curves. However the enhancement of the hump is very small and might be due to statistical fluctuations. The following table shows again the Results of the Measurements.

Sample	Q-range	range	$\alpha$	$\Delta \alpha$	$\chi^2/N$
Z1AA	0.0135 – 0.22	4.55-232	-2.340	0.017	5.70
Z1AB	0.0075 - 0.31	3.23-419	-2.341	0.013	6.98
Z3A	0.0045 – 0.42	2.38-698	-2.422	0.018	4.88
Z2B	0.0085 – 0.38	2.63-369	-2.37	0.02	5.39
Z4A	0.0095 – 0.352	2.84-331	-2.34	0.02	2.72
Z4B	0.0085 – 0.36	2.78-369	-2.350	0.017	4.06
Z5A	0.0085 – 0.3	3.33-369	-2.48	0.03	5.94
Z5B	0.0075 – 0.4	2.5-419	-2.35	0.03	7.04
Z3B	0.0135 - 0.34	2.94-233	-2.300	0.015	14.23
Z1A	0.0135 - 0.29	3.45-233	-2.423	0.012	5.05



The graph shows the values of  $\alpha$  in the power law region for each of the five states of iron-carbides, which have been investigated. It is immediately seen that different samples of the same creation method don't agree perfectly. The difference between the creation methods itself is very small and lies well within statistical fluctuations.

The value of  $\alpha$  which is -2.428(4) is unexpected and doesn't correspond to any typical shape. In general differently shaped nanoparticles give rise to different exponents. From pictures obtained by TEM and atom probe it was expected that the particles either have flat disc-like or ellipsoidal structure, which would correspond to  $\alpha$  being 2 or 4 respectively (A.Gunier, 1955). There are several possible reasons why we didn't get either. In general the most likely reason for a small difference from one of the expected exponents is polydispersity. However an exponent by -2.428(4) could only be reached by a very polydisperse material. An alternative explanation could be that the nanoparticles are porous or flaky. They would then have a fractal structure (Mandelbrot, 1977 and 1983). In SAXS one can in general interpret a non-integer exponent in the power-law as a fractal dimension (Bale, 1984). An exponent below 3 can be interpreted directly as being the mass fractal dimension of the nanoparticles (Schmidt, 1990).

## 5) Conclusions

According to our findings, there seems to be only one hump in the intensity curve due to the smaller carbides.

Also the exponent of 2.5 of the fitted power law strongly suggests that the nanoparticles are porous or flaky. Further studies should be considered to investigate the origin of the hump in more detail.

## 6) References

- 1) Harold D. Bale and Paul W. Schmidt, *Small-Angle X-Ray-Scattering Investigation of Submicroscopic Porosity with Fractal Properties*, (Physical Review Letters, Volume 53 Number 6, 1984)
- 2) A. Gunier, G. Fournet, C. B. Walker and K. L. Yudowitch, *Small-angle-Scattering of X-Rays* (Wiley, New York, 1955)
- 3) B. B. Mandelbrot, *Fractals: Form, Chance, and Dimension*, (Freeman, New York, 1977)
- 4) B. B. Mandelbrot, *The fractal geometry of nature*, (Freeman, New York, 1983)
- 5) Paul W. Schmidt, *Small-Angle Scattering Studies of Disordered, Porous and Fractal Systems*, Conference Proceedings, International Small-Angle Scattering Conference, 1990)